38

Dynamic Stability: Examples

TABLE OF CONTENTS

§38.1. Introduction

This Chapter illustrates the dynamic stability formulation of the previous Chapter by going over some classical examples of application of the linearized approach to dynamic stability. All of them are done analytically. Some are then compared with simple FEM discretizations.

§38.2. Massless Column with Point Mass and Follower Load

This benchmark problem is defined in Figure 38.1(a). An elastic, prismatic, cantilevered column is loaded by a tangential *follower* force P of constant magnitude at the tip. Axes $\{x, y\}$ are placed as shown. The column is massless and can only move in the plane of the figure. It has length L, uniform elatic modulus E and constant bending inertia I when moving laterally. The column will be modeled as a Bernoulli-Euler plane beam; thus only its lateral displacement, denoted by $v(x, \tau)$, is considered.[1] The axial motion is ignored. The point mass m is assumed to have negligible rotational inertia; whence only its translational inertia $m\ddot{v}$ (in the y direction) is considered.

For convenience the follower force magnitude is parametrized as

$$P = \lambda\, P_{Ecr} = \lambda\, \frac{\pi^2\, E\, I}{4\, L^2}. \tag{38.1}$$

in which P_{Ecr} is the Euler critical load for the static (conservative) case and λ is the control parameter. For future use we introduce additional load-related variables: k, κ, and γ, connected by the expressions

$$k = \sqrt{\frac{P}{E\, I}}, \quad \kappa = k\, L = \sqrt{\frac{P\, L^2}{E\, I}} = \frac{\pi}{2}\sqrt{\lambda}, \quad \lambda = \frac{4\kappa^2}{\pi^2}, \quad P = \kappa^2 \frac{E\, I}{L^2}, \quad \gamma = \frac{m}{k^2\, E\, I}. \tag{38.2}$$

Here κ, like λ, is dimensionless. It may be viewed as an alternative load parameter. The equilibrium state at which stability is investigated is taken to be the same as the straight-column reference configuration under initial compressive axial force P. Figure 38.1(b) depicts a possible perturbed lateral motion defined by the lateral displacements $v(x, \tau)$, which are assumed infinitesimal.

Primes will denote derivatives with respect to x.

§38.2.1. Massless Column EOM Via Spatial Second Order ODE

To derive the equation of motion (EOM) of the disturbed column we start with the Free Body Diagram (FBD) of column segment AX, in which X is at distance x from the top. See Figure 38.1(c). For infinitesimal motions $P_x = P\, \cos\theta_A \approx P$ (positive down) and $P_y = P\, \sin\theta_A \approx P\, \theta_A = P\, v'_A$ (positive along y). Taking moments with respect to X' (the displaced X) gives $M - P_x\, (v_A - v) + P_y\, x + m\, \ddot{v}_A\, x = 0$. On replacing $M = E\, I\, v''$, as well as P_x and P_y in terms of P, and moving all boundary terms to the RHS, the beam equation of motion (EOM) results:

$$E\, I\, v'' + P\, v = P\, v_A + (P\, v'_A - m\, \ddot{v}_A)\, x. \tag{38.3}$$

This is of second order in space. Dividing through by $E\, I > 0$ and replacing $k^2 = P/E\, I$ yields the canonical form

$$v'' + k^2\, v = k^2\, v_A + k^2\, (v'_A - \gamma\, \ddot{v}_A)\, x. \tag{38.4}$$

[1] Recall from the previous Chapter that τ denotes *real* time.

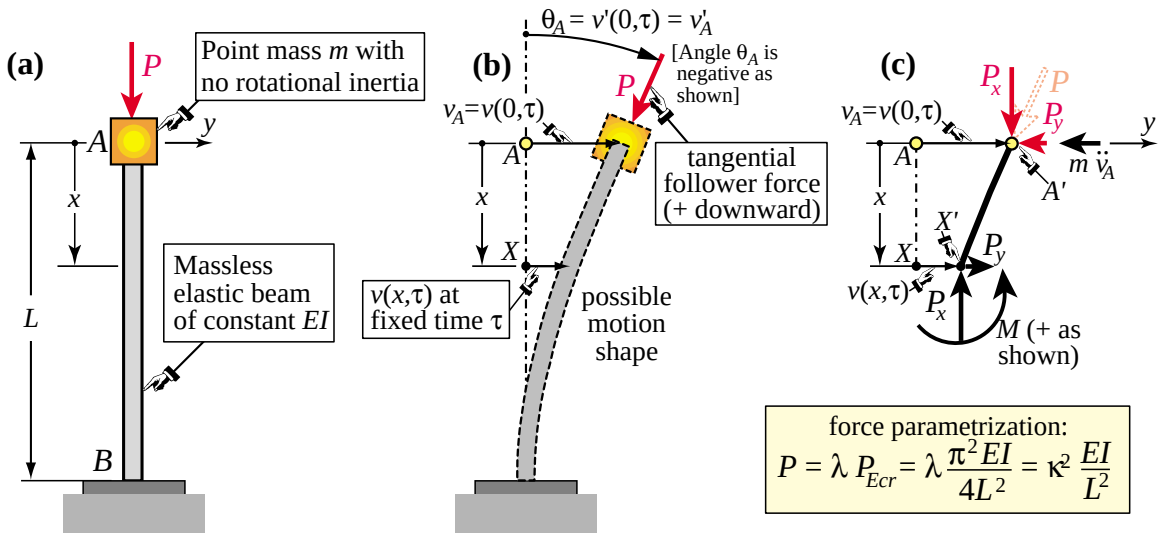

FIGURE 38.1. Massless elastic cantilevered column with point mass at free end, loaded by a constant tangential follower force P: (a) problem diagram; (b) tilted column shape (infinitesimal lateral motions are grossly exaggerated for visusization convenience); (c) Free Body Diagram (FBD) of segment AX.

in which γ is defined in (38.2). Its general solution (sum of homogeneous and particular) separates into temporal and spatial factors as

$$v(x,\tau) = w(x)\,g(\tau) = \big(A\,\sin kx + B\,\cos kx + v_A + (v'_A - \gamma\,\ddot{v}_A)\,x\big)\,g(\tau). \tag{38.5}$$

Here A and B are integration coefficients, $w(x)$ is the deflection shape function, and $g(\tau)$ is a function of time to be determined later. (The separation of variables works here because (38.4) is homogeneous in v.) The boundary conditions (BC) in space are $w(0) = w_A$, $w'(0) = w'_A$, $w(L) = 0$ and $w'(L) = 0$, in which $w_A = v_A/g(\tau)$ and $w'_A = v'_A/g(\tau)$. Application of the first two gives $A = \gamma\,\ddot{w}_A/k$ and $B = 0$, while enforcing the last two gives $w_A = \gamma\,\ddot{w}_A(L\,\cos kL - (1/k)\sin kL)$ and $w'_A = \gamma\,\ddot{w}_A(1 - \cos kL)$. On matching the top acceleration, we arrive at the temporal EOM:

$$\ddot{g} + \omega^2\,g = 0, \qquad \text{with} \quad \omega^2 = \frac{k}{\gamma\,(\sin kL - kL\,\cos kL)}. \tag{38.6}$$

Here ω is the motion frequency of the perturbed column. For subsequent studies it is convenient to use a fully dimensionless scaled form:

$$\tilde{\omega}^2 = \gamma\,k^2\,L^3\,\omega^2 = \frac{k^3\,L^3}{\sin kL - kL\,\cos kL} = \frac{\kappa^3}{\sin\kappa - \kappa\,\cos\kappa}. \tag{38.7}$$

As can be observed this derivation is messy and prone to sign errors. A more elegant procedure is described next.

§38.2.2. Massless Column EOM Via Spatial Fourth Order ODE

Some authors address this problem by starting from a EOM that is spatially of fourth order:

$$(E\,I\,v'')'' + (P\,v')' = 0, \qquad \text{for} \quad 0 \le x \le L, \tag{38.8}$$

This can be obtained by differentiating (38.3) twice with respect of x. All boundary (RHS) terms disappear.[2] Since EI and P are constant (38.8) could also be written $EI\,v^{iv} + Pv'' = 0$. Dividing through by EI and replacing $k^2 = P/EI$ we get the canonical form

$$v^{iv} + k^2\,v'' = 0, \quad \text{for} \quad 0 \le x \le L, \tag{38.9}$$

As in the previous derivation, the general solution of (38.9) is separable in space and time:

$$v(x,\tau) = w(x)\,g(\tau) = \big(A\,\sin\,kx + B\,\cos\,kx + C\,x + D\big)\,g(\tau), \tag{38.10}$$

in which A through D are integration coefficients, $w(x)$ the deflection shape function, and $g(\tau)$ is a function of time to be determined later. The coefficients A though D re to be found from the four boundary conditions (BC)

$$M(0) = 0, \quad V(0) + Pv'_A - m\,\ddot{v}_A = 0, \quad w(L) = w'(L) = 0. \tag{38.11}$$

Here $M(x)$and $V(x)$ denote the bending moment and the transverse shear force, respectively, for the Bernoulli-Euler plane beam model, which can be expressed in terms of the transverse displacement derivatives as

$$M(x) = EI\,v'', \quad V(x) = -M' - Pv' = -(EI\,v'')' - Pv' = -EI\,v''' - Pv'.$$

At the top, $V(0)$ balances the sum of the applied force $Pv'(0,\tau) = P\,v'_A$ and the inertia (D'Alembert) force $-m\ddot{v}(0,\tau) = -m\ddot{v}_A$, Therefore the second BC is simply $EI\,v'''_A - mv'_A = 0$. Substituting these expressions, the two BC at the column top become

$$w''(0) = w''_A = 0, \quad EI\,w'''_A\,g(\tau) + m\,w(0)\,\ddot{g}(\tau) = 0. \tag{38.12}$$

Replacing the four BC into the general solution (38.10) yields a linear system in the coefficients:

$$\begin{bmatrix} 0 & -k^2 & 0 & 0 \\ EI\,k^3\,g & -m\,\ddot{g} & 0 & -m\,\ddot{g} \\ \sin kL & \cos kL & L & 1 \\ k\,\cos kL & -k\,\sin kL & 1 & 0 \end{bmatrix} \begin{bmatrix} A \\ B \\ C \\ D \end{bmatrix} = \begin{bmatrix} 0 \\ 0 \\ 0 \\ 0 \end{bmatrix}, \tag{38.13}$$

For a nontrivial solution of $v(x,\tau)$ the determinant of (38.13) must vanish. This produces the homogeneous, second-order, linear EOM for the temporal function $g(\tau)$:

$$\ddot{g} + \omega^2\,g = 0, \quad \text{with} \quad \omega^2 = \frac{EI}{m}\,\frac{k^3}{\sin kL - \kappa\,\cos kL}. \tag{38.14}$$

On replacing $m = \gamma\,k^2\,EI$, this agrees fully with (38.6). The dimensionless scaled frequency $\tilde{\omega}$ is given by (38.7).

The main advantages of the fourth-order spatial form is that the derivation of (38.14) is fully automatic and easily done with a computer algebra system. The derivation presented in §38.2.1 requires a FBD, which must be done by a human[3] and is sign-error prone.

---

[2] Note that no inertia term appears in (38.8) because the column is assumed massless. That effect will come in through the transverse shear BC at $x = 0$.

[3] Computers cannot (yet) do free body diagrams; for that they would need artificial vision and understanding of Newtonian mechanics.

§38.2.3. Massless Column Stability Analysis

The general solution of the EOM $\ddot{g} + \omega^2 g = 0$ is $g(\tau) = C_1 e^{j\omega\tau} + C_2 e^{-j\omega\tau}$, in which ω is the circular frequency given by (38.6) or (38.14), and C_1 and C_2 are determined from initial conditions (IC). Since in the terminology of **?**, $p^2 = -\omega^2$ is the only characteristic root, its value alone will determine dynamic stability. Consequently the IC may be ignored. As noted at the end of §38.2.1, for visualization it is convenient to express that frequency as a dimensionless function of κ through the scaling

$$\tilde{\omega}^2 = \omega^2 \frac{m L^3}{E I} = \frac{\kappa^3}{\sin\kappa - \kappa\cos\kappa}. \tag{38.15}$$

As $P \to 0$, $\kappa \to 0$, and (38.15) approaches $0/0$. The correct limit can be obtained from the Taylor series about $\kappa = 0$:

$$\tilde{\omega}^2 = 3 + \frac{3\kappa^2}{10} + \frac{27\kappa^4}{1400} + \ldots \tag{38.16}$$

It follows that the unloaded column has a positive vibration frequency given by $\omega_0^2 = 3EI/(mL^3)$, which is a well known result,[4] and is therefore stable. As P increases, so does $\kappa = L\sqrt{P/EI}$ and the frequency goes up. The denominator of (38.15) vanishes at $\sin\kappa = \kappa\cos\kappa$, or $\tan\kappa = \kappa$. The first two positive roots of this equation are (to 16 places) $\kappa_{cr1} = 4.4934094579090641 7$, and $\kappa_{cr2} = 7.725251836937707$. The κ_{cr1} root provides the first critical load

$$P_{cr1} = \frac{\kappa_{cr1}^2\, EI}{L^2} = \frac{20.19072855642663\, EI}{L^2} = 8.18299406375318392\, P_{Ecr}. \tag{38.17}$$

in which P_{Ecr} is the Euler static critical load for a conservative load. The critical control parameter in the follower load parametrization (38.1) is $\lambda_{cr1} = 4\kappa_{cr1}^2/\pi^2 = 8.18299406375318392$. The second critical load is

$$P_{cr2} = \frac{\kappa_{cr2}^2\, EI}{L^2} = \frac{59.679515944109419\, EI}{L^2} = 24.187196778635741\, P_{Ecr}. \tag{38.18}$$

If $P_{cr1} < P < P_{cr2}$, ω^2 becomes negative indicating *divergence instability*, since $p^2 = -\omega^2$ becomes positive real. If $P_{cr2} < P < P_{cr3}$, ω^2 again becomes positive, and so on. These regions may be observed in the diagram of ω^2 versus κ shown in Figure 38.2(a). A variant of the "root amplitude plots" described in **?** is shown in Figure 38.2(b), which graphs λ versus $\log(|\omega|)$. This is called a frequency-versus-load response plot or FLP. Use of the log scale for $|\omega|$ clearly marks where infinite frequency "resonances" occur.[5]

This peculiar form of stable-to-unstable transition: "divergence at infinity," is due to ignoring the distributed mass of the column. Accounting for it changes the transition to a more classical form of finite-frequency-pair coalescence (flutter), as in the Beck's column benchmark covered in §38.3.

---

[4] That is the natural frequency of an unforced, massless cantilever beam with a point mass at the free end.

[5] Plots of this nature in log-log form are commonly used in dynamics and control, in which applied loads are often harmonic in time. The so-called "frequency response plots" or FRP, display log of response amplitude logs versus log of forcing frequency.

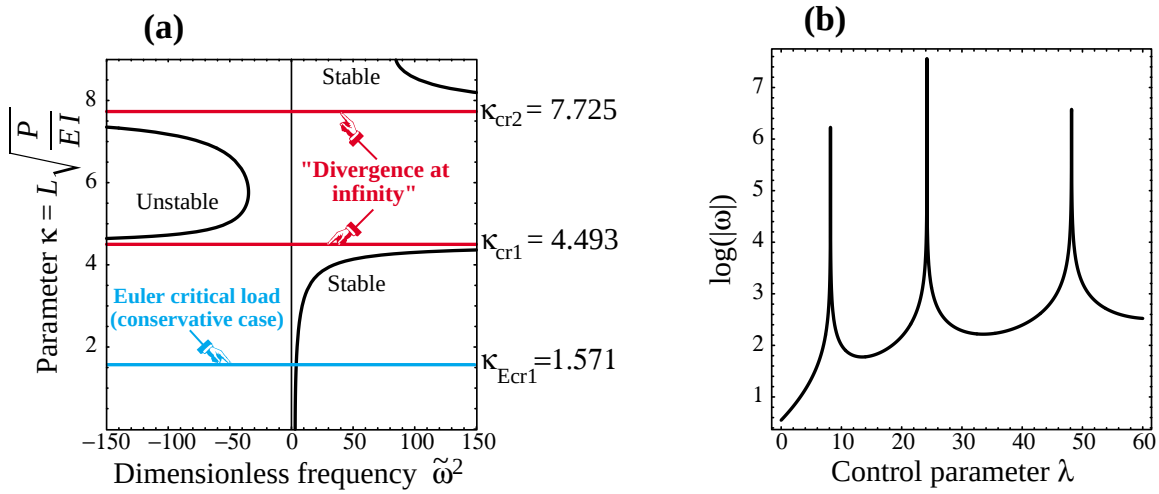

FIGURE 38.2. Dynamic stability diagrams for problem of Figure 38.1: (a) plot of dimensionless squared frequency $\tilde{\omega}^2$ versus parameter $\kappa = L\sqrt{P/EI}$; (b) frequency-versus-load plot (FLP) graphing the control parameter λ defined in (38.1) versus $\log(|\omega|)$. In the latter, critical values of λ occur at the clearly visible "resonance" peaks.

Remark 38.1. Can this structure lose stability under static conditions? That would require, using the zero frequency condition (equivalent to the singular stiffness criterion), that $\omega = 0$ for some $\lambda > 0$. It is easily verified, however, that the expression of ω^2 given by (38.15) does not vanish for any positive value of $\kappa = \pi\sqrt{\lambda}/2$. Thus only dynamic instability is possible. This property: inexistence of static buckling configurations, is typical of many follower load problems.

§38.2.4. Massless Column: FEM Solution

The problem of Figure 38.1 is now idealized with FEM discretizations of N_e equal length Bernoulli-Euler beam elements, where N_e varies from 1 through 32 in doubling steps. Meshes with 1, 2 and 4 elements are pictured in Figure 38.3(a). the CR geometric stiffness of Chapter 11. This discretizaton has two degrees of freedom at each node n: the lateral translation v_n and the rotation θ_n about z. The clamping condition at the base is imposed by eliminating those two DOF from the FEM equations.

To set up the characteristic eigensystem (37.4) we need the mass matrix $\mathbf{M}$ and the tangent stiffness matrix $\mathbf{K} = \mathbf{K}_M + \mathbf{K}_G + \mathbf{K}_L$ at the reference configuration under initial compressive force P.

Example 38.1. Let us work out the one element model. The necessary FEM matrices are

$$\mathbf{M}^e = \begin{bmatrix} m & 0 & 0 & 0 \\ 0 & 0 & 0 & 0 \\ 0 & 0 & 0 & 0 \\ 0 & 0 & 0 & 0 \end{bmatrix}, \quad \mathbf{K}_M^e = \frac{EI}{L^e}\begin{bmatrix} 12/(L^e)^2 & 6/L^e & -12/(L^e)^2 & 6/L^e \\ 6/L^e & 4 & -6/L^e & 2 \\ -12/(L^e)^2 & -6/L^e & 12/(L^e)^2 & -6/L^e \\ 6/L^e & 2 & -6/L^e & 4 \end{bmatrix},$$

$$\mathbf{K}_G^e = -\frac{P}{30\,L^e}\begin{bmatrix} 36 & 3\,L^e & -36 & 3\,L^e \\ 3\,L^e & 4\,(L^e)^2 & -3\,L^e & -(L^e)^2 \\ -36 & -3\,L^e & 36 & -3\,L^e \\ 3\,L^e & -(L^e)^2 & -3\,L^e & 4\,(L^e)^2 \end{bmatrix}, \quad \mathbf{K}_L^e = \begin{bmatrix} 0 & -P & 0 & 0 \\ 0 & 0 & 0 & 0 \\ 0 & 0 & 0 & 0 \\ 0 & 0 & 0 & 0 \end{bmatrix}, \tag{38.19}$$

$$\mathbf{u}^e = [\, v_1 \quad \theta_1 \quad v_2 \quad \theta_2 \,]^T .$$

in which $L^e = L$ denotes the element length. (The mass and load stiffness matrix given above are valid for element $e = 1$; for discretizations with more than one element those matrices vanish for $e = 2, 3 \ldots$; see the

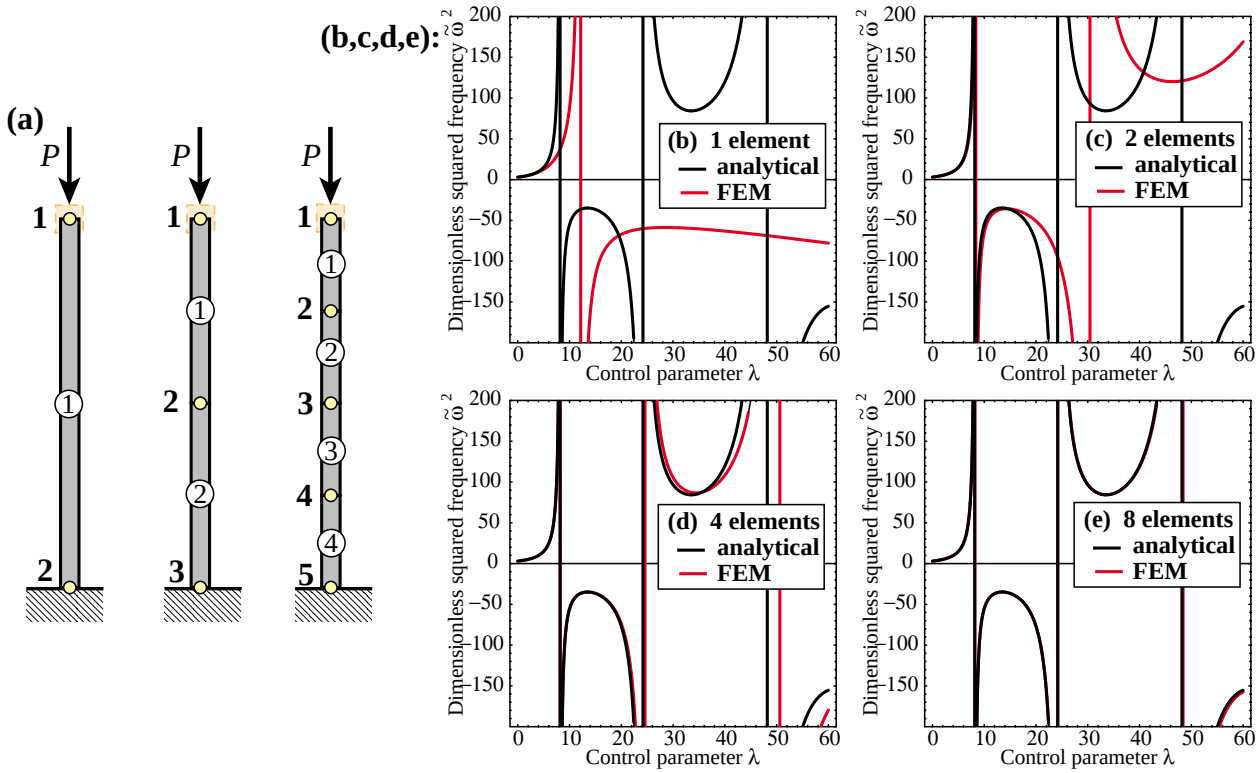

FIGURE 38.3. Dynamic stability analysis for problem of Figure 38.1 with the Finite Element Method (FEM): (a) sketch of FEM meshes with 1, 2 and 4 elements along column length; (b–e) plots (red) of $\tilde{\omega}^2$ versus control parameter λ obtained from discretizations with 1, 2, 4 and 8 elements, respectively, compared to analytical solution (black).

next example.) The material and geometric stiffnesses are those fo the Bernoulli-Euler CR plane beam derived in Chapter 11. The clamped condition at node 2 is applied by removing v_2 and θ_2 from $\mathbf{u}^e$. The resulting eigensystem is

$$\mathbf{A}\,\mathbf{z}_i = (p_i^2\,\mathbf{M}+\mathbf{K})\,\mathbf{z}_i = \left(p_i^2\begin{bmatrix} m & 0 \\ 0 & 0\end{bmatrix} + \begin{bmatrix} \frac{12EI}{L^3}-\frac{6P}{5L} & \frac{6EI}{L^2}-\frac{11P}{10} \\ \frac{6EI}{L^2}-\frac{P}{10} & \frac{4EI}{L}-\frac{2PL}{15}\end{bmatrix}\right)\begin{bmatrix} v_1 \\ \theta_1\end{bmatrix}_i = \begin{bmatrix} 0 \\ 0\end{bmatrix}. \tag{38.20}$$

Note the unsymmetry of $\mathbf{K}$. The determinant of the matrix combination $\mathbf{A} = p_i^2\mathbf{M}+\mathbf{K}$ is

$$\det(\mathbf{A}) = \frac{720\,(EI)^2 + L^4\,P\,(3\,P - 8\,m\,L\,p_i^2) + 48\,EI\,L^2\,(P+5\,m\,L\,p_i^2)}{60\,L^4}. \tag{38.21}$$

Equating this to zero and solving for p_i^2 yields the only root

$$p_1^2 = \frac{720(EI)^2 + 48\,EI\,L^2\,P + 3L^4\,P^2}{8\,m\,L^3\big[PL^2 - 30\,EI\big]} \tag{38.22}$$

Notethis FEM discretization has only *one* finite eigenroot. Reason: the rotational inertia associated with θ_1 is zero. The numerator of (38.22) has only complex roots and thus cannot vanish for any real value of P. We can therefore expect only one critical load, associated with an infinite frequency. This is obtained by setting

the denominator of (38.22) to zero, which yields

$$P_{cr1} = \frac{30\,EI}{L^2}. \tag{38.23}$$

The result is independent of m. Transition to instability occurs by divergence at ∞. The *Mathematica* plot of exact (analytic) versus FEM, as it appears in a frame of Figure 38.3, is done by

```
\[Omega]\[Omega]=-pp/.{m->1,EI->1,L->1,P->\[Lambda]*Pi^2/4};
\[Omega]\[Omega]=N[\[Omega]\[Omega]];
\[Kappa]=(Pi/2)*Sqrt[\[Lambda]];
\[Omega]\[Omega]exact=\[Kappa]^3/(Sin[\[Kappa]]-\[Kappa]*Cos[\[Kappa]]);
dfun=$DisplayFunction; If [$VersionNumber>=6.0, dfun=Print];
Plot[{\[Omega]\[Omega],\[Omega]\[Omega]exact},{\[Lambda],0,60},Frame->True,
     PlotStyle->{{AbsoluteThickness[2],RGBColor[1,0,0]},
     {AbsoluteThickness[2],RGBColor[0,0,0]}},
     ImageSize->300,PlotRange->{-200,200},
     PlotPoints->400,AspectRatio->1,DisplayFunction->dfun];
```

in which pp is the characteristic root (38.22).

Example 38.2. Next, lets work out the two element case. The material and geometric stiffness matrices are similar to those of the previous example, in which L^e is now $L/2$. An adjustment is required, however, for the mass matrix $\mathbf{M}^e$ and the load stiffness matrix $\mathbf{K}^e_L$ for $e = 2$: both are null 4×4 matrices since the point mass m and the applied load P act on node 1, which is outside element 2. The master $\mathbf{K}$ and $\mathbf{M}$ are now 6×6. They are reduced to 4×4 by removing freedoms v_3 and θ_3 at the fixed node 3, whence the DOF vector is just $\mathbf{z} = [\, v_1 \;\; \theta_1 \;\; v_2 \;\; \theta_2 \,]^T$. Setting $L = EI = m = 1$ for display convenience, the reduced stiffness and mass matrices are

$$\mathbf{K} = \begin{bmatrix} 96 - \frac{12\,P}{5} & 24 - \frac{11\,P}{10} & \frac{12\,(-40+P)}{5} & 24 - \frac{P}{10} \\ 24 - \frac{P}{10} & 8 - \frac{P}{15} & -24 + \frac{P}{10} & 4 + \frac{P}{60} \\ \frac{12\,(-40+P)}{5} & -24 + \frac{P}{10} & \frac{-24\,(-40+P)}{5} & 0 \\ 24 - \frac{P}{10} & 4 + \frac{P}{60} & 0 & 16 - \frac{2\,P}{15} \end{bmatrix}, \quad \mathbf{M} = \begin{bmatrix} 1 & 0 & 0 & 0 \\ 0 & 0 & 0 & 0 \\ 0 & 0 & 0 & 0 \\ 0 & 0 & 0 & 0 \end{bmatrix}. \tag{38.24}$$

The resulting eigensystem is $(p_i^2\,\mathbf{M} + \mathbf{K})\,\mathbf{z}_i = \mathbf{0}$. The determinant of $\mathbf{A} = p_i^2\,\mathbf{M} + \mathbf{K}$ is

$$\det(\mathbf{A}) = \frac{1}{1200}\left(3\,(3840 + P\,(64 + P))^2 - 16\,(-921600 + P\,(61440 + P\,(-880 + 3\,P)))\,p_i^2\right). \tag{38.25}$$

which as in the previous example is linear in p_i^2. Equating to zero and solving yields the only characteristic root

$$p_1^2 = \frac{3\,(3840 + 64\,P + P^2)^2}{16\,(-921600 + 61440\,P - 880\,P^2 + 3\,P^3)}, \tag{38.26}$$

The numerator has only complex roots and so it cannot vanish for any real value of P. Thus we can expect only critical loads associated with an infinite frequency, i.e., divergence at infinity. These are obtained by setting the denominator of (38.26) to zero. This gives three real roots, which on restoring EI and L are

$$P_{cr1} = \frac{20.7088\,EI}{L^2}, \quad P_{cr2} = \frac{75.1015\,EI}{L^2}, \quad P_{cr3} = \frac{197.523\,EI}{L^2}. \tag{38.27}$$

Plotting p_1^2 versus the exact (analytical) value can be done through the same script shown in the previous example.

Table 38.1. FEM Results For Massless Column: Dynamic Versus Static

Elements	P_{cr1}^{dyn}	P_{cr2}^{dyn}	P_{cr3}^{dyn}	P_{cr1}^{sta}	P_{cr2}^{sta}	P_{cr3}^{sta}
1	30.0000			2.4859		
2	20.7088	75.1015	197.523	2.4688	22.9462	77.0631
4	20.2322	60.6353	124.886	2.4675	22.2621	62.7526
8	20.1935	59.7481	119.419	2.4674	22.2068	61.7609
16	20.1909	59.6840	118.935	2.4674	22.2066	61.6899
32	20.1907	59.6798	118.902	2.4674	22.2066	61.6853
analytical	20.1907	59.6795	118.852	2.4674	22.2066	61.6850

Numbers in table are the coefficients of EI/L^2 for the listed critical loads.

The one-element result (38.23) for P_{cr} is 50% higher than the analytical value 20.1907 EI/L^2 given in (38.17). The two-element result (38.27) is 2.6% higher for P_{cr1} but way off for the next two. The accuracy can be improved by increasing the number of elements. Results obtained with 1 through 32 elements for first 3 critical dynamic loads, labeled P_{cri}^{dyn}, ($i = 1, 2, 3$), are tabulated in columns 2 through 4 of Table 38.1. Convergence is seen to be satisfactory, at least for the first critical load.

For comparison, columns 5 through 7 of that Table list the 3 lowest *static* critical loads computed by the FEM models for the *conservative* case, in which load P stays vertical. Those can be easily obtained by setting $\mathbf{K}_L = \mathbf{0}$ in the eigensystem $(p_i^2\mathbf{M} + \mathbf{K})\,\mathbf{z}_i = \mathbf{0}$ and getting the roots of the numerator of the p_i^2 roots.[6] It can be noted that convergence to the static critical loads is faster, since $N_e = 8$ already provides 3-5 places of accuracy in the first 3 critical loads. (Note that $P_{cr1}^{sta} = P_{Ecr} = \frac{1}{4}\pi^2\,EI/L^2 \approx 2.4674\,EI/L^2$, etc.) In all cases convergence is from above.

A more comprehensive view of FEM accuracy can be gleaned from the four $\tilde{\omega}^2$ versus λ plots shown in Figure 38.3(b–e). These compare FEM solutions for 1, 2, 4 and 8 elements with the analytical result (38.15) as λ varies. See legend of that figure for explanation.

Remark 38.2. Conventional flutter cannot occur in this problem since it has only one dynamical degree of freedom (DOF): the lateral motion of the point mass. Therefore coalescence of two frequencies cannot happen. (The FEM model has multiple DOF, but only one endowed with inertia.)

.

[6] This is effectively an aplication of the zero frequency condition, which is equivalent to both the singular stiffness and the divergence-at-zero criteria.

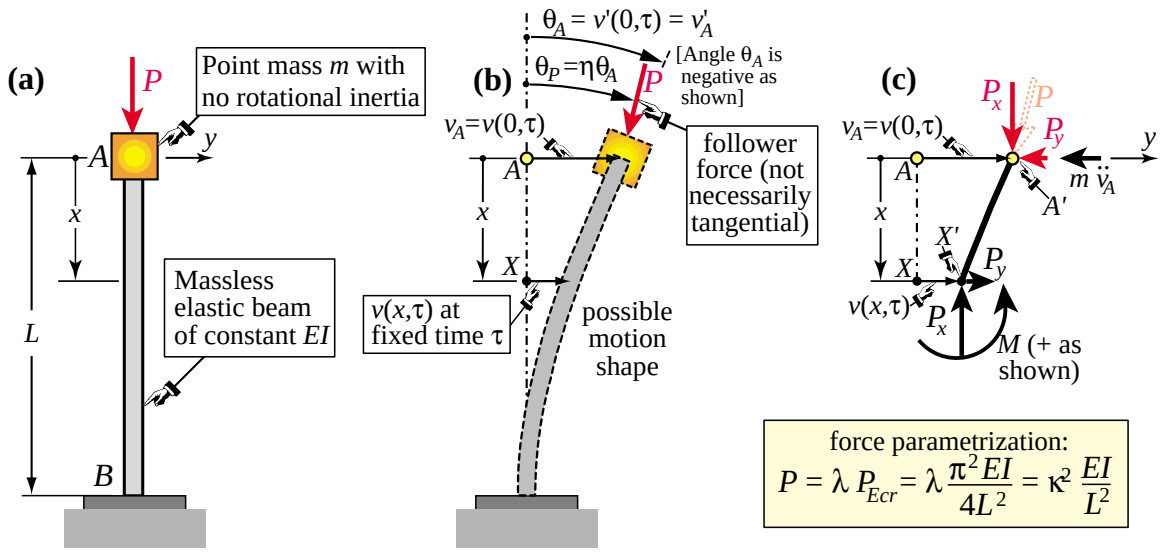

FIGURE 38.4. Massless elastic cantilevered column with point mass at free end, loaded by an *tilt parametrized* constant tangential follower force P: (a) problem diagram; (b) tilted column shape (infinitesimal lateral motions are grossly exaggerated for visualization convenience); (c) Free Body Diagram (FBD) of segment AX.

§38.2.5. Massless Column Under Tilt-Parametrized Follower Force

We slightly generalize the foregoing problem as pictured in Figure 38.4. The only difference is that the angle θ_P that the applied end force makes with the tip angle θ_A is now $\eta\,\theta_A$, in which η is an arbitrary real number. If $\eta = 1$ we recoved the previous example whereas if $\eta = 0$ the load remains vertical and therefore conservative. Thus this generalization furnishes a simple example of a system that may lose stability statically or dynamically depending on a parameter. The interesting question is: at which η does the transition occur?

The analytical treatment is quite similar to that presented in §38.2.1 through §38.2.3 for the $\eta = 1$ case, and is relegated to an Exercise. The key result is that the phyical and scaled dimensionless frequencies become

$$\omega^2 = \frac{EI}{m}\,\frac{k^3\left(\eta + (1-\eta)\cos kL\right)}{\sin kL - \kappa\cos kL}, \quad \tilde{\omega}^2 = \frac{m\,L^3}{EI}\,\omega^2 = \frac{\kappa^3\left(\eta + (1-\eta)\cos\kappa\right)}{\sin\kappa - \kappa\cos\kappa}. \tag{38.28}$$

The denominator is the same for all η, whence the stability loss due to divergence at infinity is identical to that found in §38.2.3. But now the numerator may vanish if $\eta \le \frac{1}{2}$. This happens if

$$\kappa_{cr} = \arccos\left(\frac{\eta}{\eta - 1}\right). \tag{38.29}$$

This indicates loss of stability due to divergence at zero, which may also be obtained through static criteria. Since the arccos function is multivalued, (38.29) gives an infinite number of roots for a given $\eta \le \frac{1}{2}$. Of these only the principal value one as well as neighboring roots are of physical interest. If $\eta > \frac{1}{2}$, (38.29) gives only complex roots so stability loss can only be dynamic in nature.

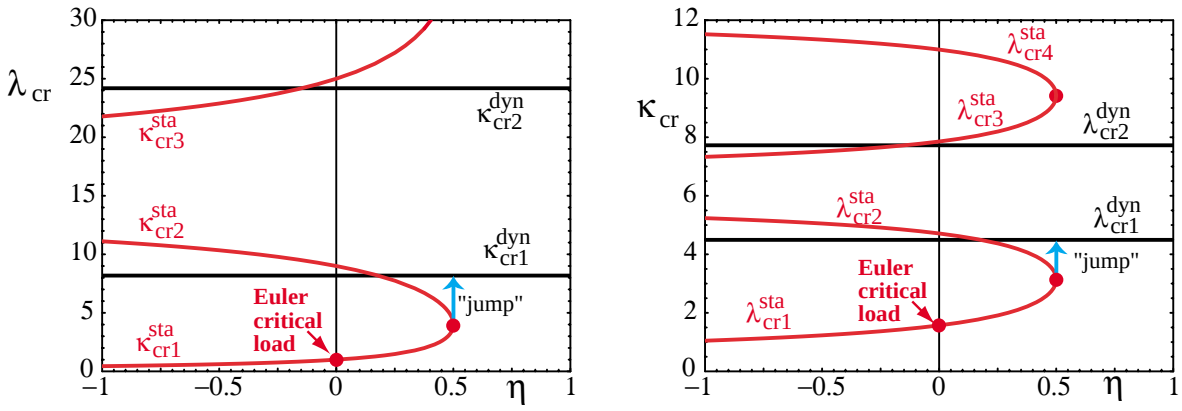

FIGURE 38.5. Critical loads of the tilt-parametrized massless cantilever shown in Figure 38.4 as a function of parameter η; (a) control parameter κ versus η and (b) control parameter λ versus η; recall that $\kappa = (\pi/2)\sqrt{\lambda}$ whereas $\lambda = 4\kappa^2/\pi^2$. Static and dynamic critical load branches marked in red and black, respectively. Here "static" and "dynamic" mean critical event occurrence by divergence at zero and divergence at infinity, respectively.

The results are summarized in Figure 38.5, which shows the critical loads as either κ_{cr} versus η or λ_{cr} versus η. Critical load branches lying in the plotted region are shown in red (static) or black (dynamic). The latter do not depend on η since the denominator of the critical frequencies pictured in (38.28) does not depend on it.

The sudden static-to-dynamic "critical load jumps" at $\eta = 1/2$ is worth noting. This unexpected feature is actually a consequence of the extreme mass idealization of the problem. For example, if the point mass is assigned a small rotatory inertia, the transition-to-instability is smoothed out.

Remark 38.3. The analytical solution plot of κ_{cr} (first 4 branches) versus η, which appears in red in the left side of Figure 38.5 may be done as follows (*Mathematica* versions 8 or 9):

```
ClearAll[z,\[Eta]];
ArcCosFourBranches[z_]:=Module[{z1=ArcCos[z]},
   Return[{z1,2*Pi-z1,2*Pi+z1,4*Pi-z1}]];
\[Kappa]crstatab=ArcCosFourBranches[\[Eta]/(\[Eta]-1)];
Plot[Evaluate[\[Kappa]crstatab],{\[Eta],-1,1},PlotRange->{{-1,1},{0,30}},
   ImageSize->350,AspectRatio->3/4,PlotStyle->{{AbsoluteThickness[2],
   RGBColor[1,0,0]}},Frame->True,DisplayFunction->Print];
```

§38.3. Beck's Column

This is a prismatic cantilever column loaded by a tip follower force P, shown in Figure 38.6. The main difference from that pictured in Figure 38.1 is that the column is no longer massless. A uniformly distributed mass is assumed, and there is no point mass at the top. This configuration was worked out first by Beck in a 1952 paper [67] and hence it is colloquially dubbed Beck's column. An analytical dynamic stability analysis may be found in the books of Bolotin [101, §2.2] and Timoshenko-Gere [775, §2.21], and is not repeated here. According to [775] the first critical load is found to be at

$$P_{cr1} = \frac{2.008\,\pi^2 E I}{L^2} = \frac{19.82 E I}{L^2}. \tag{38.30}$$

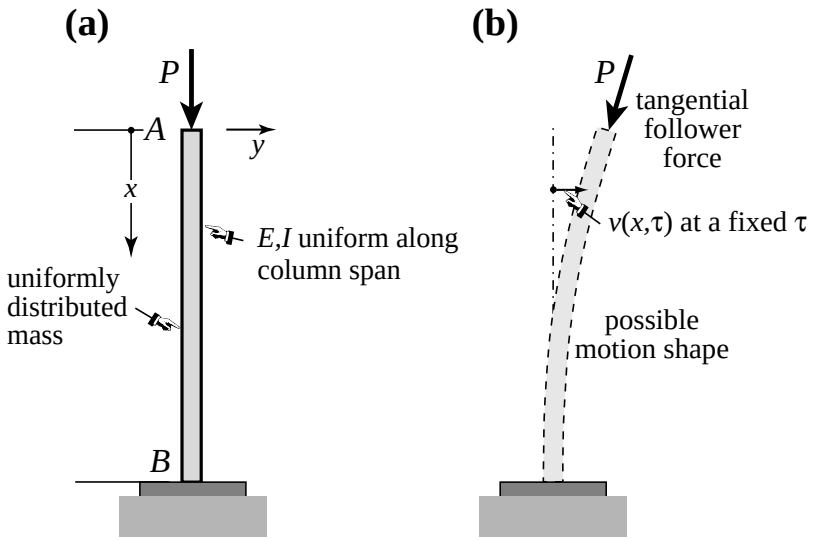

FIGURE 38.6. Beck's column benchmark: a prismatic cantilever beam with uniformly distributed mass and subject to follower point load at tip: (a), reference configuration; (b) tilted column shape.

This is not too different from the first critical load for the massless-columnwith-end-point-mass given in (38.17), and over 8 times the Euler critical load. But the loss of instability is through conventional flutter produced by a two-frequency coalescence. Here only the FEM analysis is briefly reported in the next subsection, and then worked out in detail for the one-element discretization.

§38.3.1. FEM Analysis of Beck's Column

Discretizations of 1, 2 and 4 elements similar to those pictured in Figure 38.3(a) were set up. The material and geometric and load-stiffness components of the tangent stiffness matrix in the reference configuration are exactly the same as used for the massless column example in §38.2.4. Two types of BE-beam element mass matrices were used to capture the distributed mass effect:

Lumped Mass Matrix. A diagonal mass matrix $\mathbf{M}_L$ built by halving the total mass of the element, and assigning it to each end translational DOF. Both node rotational masses are set to zero. The number of finite p_i^2 characteristic eigenroots is N_e, where N_e is the number of elements.

Optimal Mass Matrix. A nondiagonal mass matrix $\mathbf{M}_{opt}$ constructed by taking the average of the well known consistent mass matrix $\mathbf{M}_C$ and the lumped mass matrix $\mathbf{M}_L$ described above.[7] The number of finite p_i^2 characteristic eigenroots is $2N_e$, where $2N_e$ is the number of elements.

Selected results from the FEM analysis are pictured in Figures 38.7 and 38.8. The analytical flutter load is not captured very accurately by these discretizations. Results will be discussed in more detail during the next offering of this course; furthermore the figures will be better labeled.

§38.3.2. Analysis of Beck's Column With One-Element Discretization

We evaluate all FEM matrices at the reference configuration, subjected to the compressive load P. One apparent complication with respect to the FEM analysis of the massless column is that the axial displacement of the column (that along the x axis) is initially taken into account, and so one

[7] For a more detailed discussion of this topic, see [265, Chapter 33].

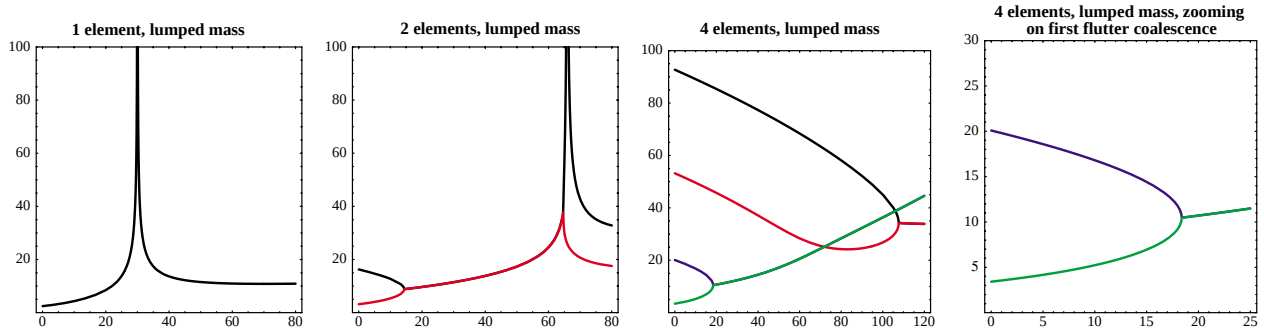

FIGURE 38.7. Beck's column results from FEM analysis using the lumped mass matrix: (a) one element; (b) two elements; (c) four elements; (d) four elements, zooming on the lowest frequency coalescent point, which signals the occurrence of flutter. Horizontal axis: axial load scaled by EI/L^2; vertical axis: moduli of characteristic roots p_i.

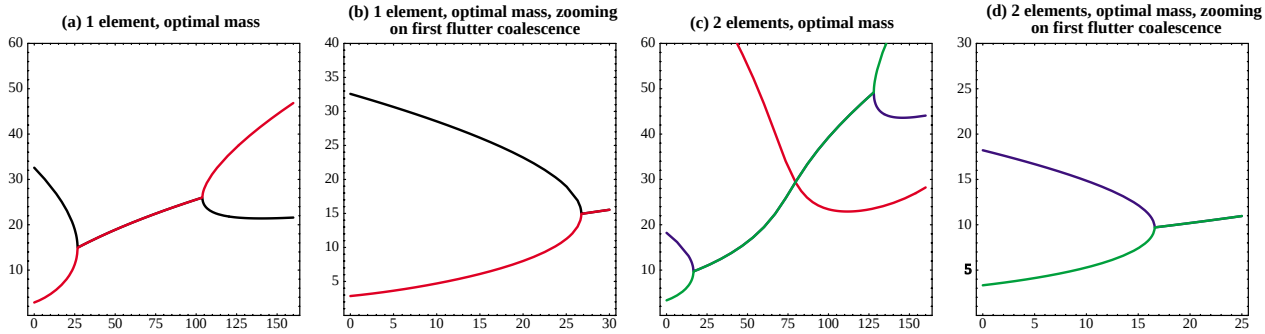

FIGURE 38.8. Beck's column results from FEM analysis using the optimal mass matrix: (a) one element; (b) one elements zooming on the first frequency coalescence; (c) two elements; (d) four element zooming on the lowest frequency coalescent point. Horizontal axis: axial load scaled by EI/L^2; vertical axis: moduli of characteristic roots p_i.

starts with are three DOF per node. For the one-element, two-node case there are initially six DOF, which are reduced to three on removing the DOF of the fixed end (node 2). The surviving DOF at the top (node 1) will be denoted by (u_1, v_1, θ_1). But we will see below that u_1 can be ignored whereas θ_1 can be eliminated by static condenstaion if the mass matrix of of lumped form.

The tangent stiffness matrix is the sum of the material, geometric and load stiffness matrices. Upon removal of the fixed-end DOF these are given by

$$\mathbf{K}_M = \begin{bmatrix} \frac{EA}{L} & 0 & 0 \\ 0 & \frac{12EI}{L^3} & \frac{6EI}{L^2} \\ 0 & \frac{6EI}{L^2} & \frac{4EI}{L} \end{bmatrix}, \quad \mathbf{K}_G = -\frac{P}{30L}\begin{bmatrix} 0 & 0 & 0 \\ 0 & 36 & 3L \\ 0 & 3L & 4L^2 \end{bmatrix}, \quad \mathbf{K}_L = P\begin{bmatrix} 0 & 0 & 0 \\ 0 & 0 & 1 \\ 0 & 0 & 0 \end{bmatrix}. \tag{38.31}$$

Here L is the column length, E the elastic modulus, A the cross section area, and I the bending moment of inertia of the cross section with respect to z. The material and geometric stiffnesses are those of the TL Bernoulli-Euler beam, augmented with the standard (uncoupled) bar stiffness

For the mass matrix we take the lumped-mass version, which is

$$\mathbf{M}_L = \begin{bmatrix} m & 0 & 0 \\ 0 & m & 0 \\ 0 & 0 & 0 \end{bmatrix}, \quad \text{in which} \quad m = \tfrac{1}{2}\rho\, g\, A\, L. \tag{38.32}$$

Here ρ and g denote the mass density and acceleration of gravity, respectively. Physically m is one half of the total element mass, which is assigned to node 1. The characteristic dynamic equation is

$$\left(p_i^2\, \mathbf{M}_L + \mathbf{K}\right)\, \mathbf{z}_i = \mathbf{0}. \tag{38.33}$$

in which $\mathbf{K} = \mathbf{K}_M + \mathbf{K}_G + \mathbf{K}_L$. At first sight this appears to be a three-DOF system. However, the first dynamic equation in u_1 uncouples and has no effect in the analysis, whence it can be discarded. The last (third) equation is static in nature because the rotational mass is zero. Thus, we can solve for θ_1 in favor of v_1:

$$\theta_1 = \frac{N}{D}\, v_1, \quad \text{in which} \quad N = -\frac{6EI}{L^2} + \frac{P}{10}, \quad D = \frac{4EI}{L} - \frac{4PL}{30}. \tag{38.34}$$

in which N and D denote the numerator and denominator, respectively, of the relation that links θ_1 to v_1. Inserting this into (38.33) the characteristic eigenproblem reduces to just one equation:

$$\left(p^2\, m + \frac{12EI}{L^3} - \frac{6EI}{L^2}\,\frac{N}{D} - \frac{36P}{30L} + 3L\frac{N}{D}\frac{P}{30L} + P\frac{N}{D}\right)\, v_1 = 0. \tag{38.35}$$

One of the bending eigenvalues p^2 of the characteristic eigensystem (38.33) is always ∞ because the rotational mass is zero. The finite p^2 becomes infinite if $D = 0$ while $N \neq 0$. Thus the critical load for divergence-at-infinity is

$$P_{cr} = \frac{30EI}{L^2}, \tag{38.36}$$

which is about 50% in error with respect to the analytical value $19.82\, EI/L^2$ quoted earlier

Notes and Bibliography

The examples presented in this Chapter are standard benchmarks in most books that treat dynamic stability of structures. The massless column under follower force is worked out in [65] and [101]. The tilt-parametrized generalization is covered in [570], but the analysis is incomplete since the authors forget that the arccos function is multivalued, and truncate the primary static branch at $\eta = 1/2$ (where it actually has a turning point). The Beck's column benchmark is succintly covered in [775] and in more detail in [101].

Homework Exercises for Chapter 38

Dynamic Stability: Examples

EXERCISE 38.1 (A+C:25) This Exercise studies the stability of the "follower load" nonconservative system shown in Figure E38.1.

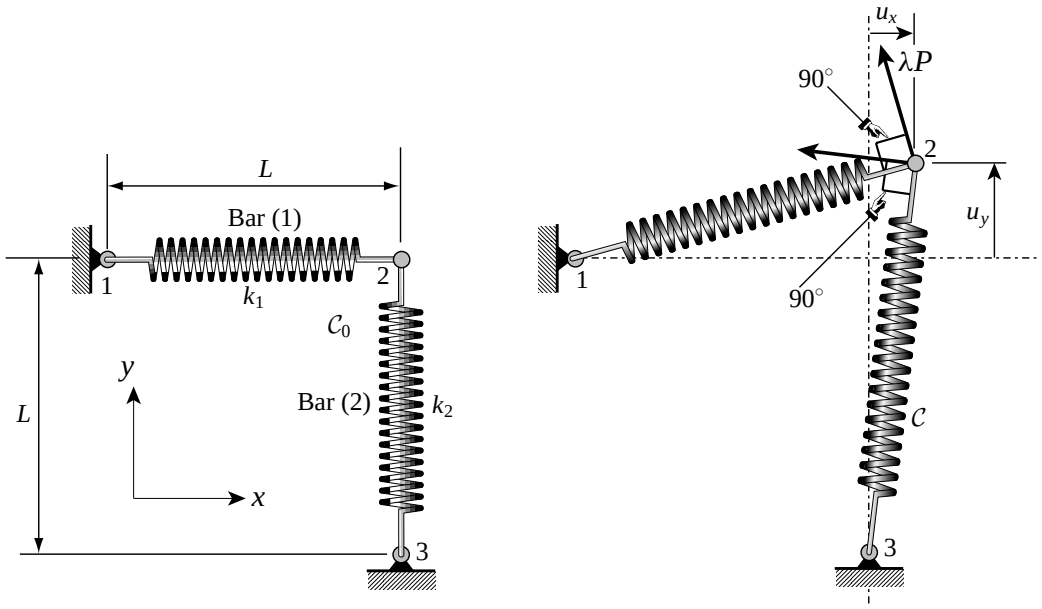

FIGURE E38.1. Structure for Exercise 38.1.

Two elastic bars, (1) and (2), are supported at 1 and 3 and hinged at 2. The bars have length L, axial stiffnesses k_1 and k_2, respectively, and can only move in the x, y plane. Bar (1) is loaded at node 2 by a force λP_1, directed upwards, that stays normal to bar (1) as it displaces. Bar (2) is loaded at node 2 by a force λP_2, directed leftwards, that stays normal to bar (2) as it displaces.

For the present exercise set $P_1 = P_2 = P$. Furthermore the following simplifying assumptions are to be made:

(A1) The displacements from the reference configuration are so small that $\mathcal{C} \equiv \mathcal{C}_0$ insofar as setting up the stability eigensystem[8]

(A2) The contribution of the geometric stiffness is neglected.

(a) Show that under the simplifying assumptions (A1)–(A2), the tangent stiffness at $\mathcal{C} \equiv \mathcal{C}_0$ in terms of the two degrees of freedom $u_x = u_{x2}$ and $u_y = u_{y2}$, is

$$\mathbf{K} = \begin{bmatrix} k_1 & 0 \\ 0 & k_2 \end{bmatrix} + \frac{\lambda P}{L} \begin{bmatrix} 0 & 1 \\ -1 & 0 \end{bmatrix}. \tag{E38.1}$$

The first component of $\mathbf{K}$ is the material stiffness whereas the second component is the load stiffness. Hint for the latter: use the results of Remark 33.4

[8] This is similar to LPB (Chapters 24-25), but here a dynamic analysis is involved.

(b) The linearized dynamic eigenproblem (33.4) is

$$(p_i^2\mathbf{M} + \mathbf{K})\mathbf{z}_i = \mathbf{0}, \qquad i = 1, 2. \tag{E38.2}$$

The exponents p_i (the square roots of p_i^2) are generally complex numbers:

$$p_i = \alpha_i + j\omega_i, \tag{E38.3}$$

in which α and ω are the real and imaginary part of p_i, respectively, $\mathbf{z}_i$ are associated eigenmodes, and $\mathbf{M}$ is the diagonal mass matrix

$$\mathbf{M} = \begin{bmatrix} M & 0 \\ 0 & M \end{bmatrix}, \tag{E38.4}$$

where M is the lumped mass at node 2 (half of the sum of the bar masses). By appropriate normalization show that the eigenproblem can be reduced to the *dimensionless* form

$$\left\{ \bar{p}^2 \begin{bmatrix} 1 & 0 \\ 0 & 1 \end{bmatrix} + \begin{bmatrix} \kappa & 0 \\ 0 & 1 \end{bmatrix} + \bar{\lambda} \begin{bmatrix} 0 & 1 \\ -1 & 0 \end{bmatrix} \right\} \bar{\mathbf{z}}_i = \mathbf{0}, \tag{E38.5}$$

in which $\kappa = k_1/k_2$, $\bar{p}$ and $\bar{\lambda}$ are dimensionless.

(c) Show that the critical positive $\bar{\lambda}_{cr}$ at which the eigenvalues $\bar{p}_i^2$ coalesce is given by the relation

$$\bar{\lambda}_{cr} = \frac{|1 - \kappa|}{2}. \tag{E38.6}$$

Further show that if $\bar{\lambda} > \bar{\lambda}_{cr}$ the roots $\bar{p}_i$ become complex and hence explain whether loss of stability occurs. Is it divergence or flutter?

(d) For $\kappa = 0.01$, 1.0, 4.0 and 100 plot the dependence of $|\bar{p}_i|$ $(i = 1, 2)$ (where $|.|$ denotes the modulus of a complex number) on λ using

$$|\bar{p}|/\sqrt{\kappa}, \qquad \lambda/\sqrt{\kappa}, \tag{E38.7}$$

as vertical and horizontal axes, respectively. Go from $\lambda = 0$ up to $2\lambda_{cr}$ or 1.0, whichever is greater, and use sufficient steps to get reasonable graphical accuracy.

EXERCISE 38.2 (A+C:25) Do the previous exercise removing assumption (A2), that is, considering now the effect of the geometric stiffness $\mathbf{K}_G$ but still assuming $\mathcal{C} \equiv \mathcal{C}_0$. Is there any difference with the critical load result (E38.6) ?

EXERCISE 38.3 (A+C:25) Complete derivations for the tilt-parametrized version of the massless cantilevered column with tip point mass and end-laoded by angle-parametrized follower load treated in §38.2.5 and pictured in Figure 38.4. Items:

(a) Derive the frequency expression given in (38.28) and the result (38.29) for the static critical loads. For the EOM derivation the 4th order ODE method used in §38.2.2 is recommented, changing the transverse shear BC to $E\,I\,w_A''' \,g + m\,\ddot{g} w_A + (1-\eta) P\, w_A' \,g = 0$.

(b) Confirm the stability diagram of Figure 38.5.

(c) Explain the physical reason why the Euler critical load (marked by a red dot in Figure 38.5) is raised if $\eta > 0$ but reduced if $\eta < 0$ (Hint: does the follower load help to resist buckling?)

(d) Find the critical loads with a one-element discretization, keeping η as variable. Reuse the mass and stiffness matrices of §38.2.4, adjusting $\mathbf{K}_L$ appropriately. Compare your results to those of Figure 38.5.

EXERCISE 38.4 (A:25) Redo the previous exercise for a one-element discretization if the line of action of the applied end load is forced to pass through the cantilever root. Does the transition to instabiliy happen statically or dynamically? (Hint: the applied loading becomes conservative).